

# Universality of Dicke superradiance in atomic arrays

Stuart J. Masson<sup>1,\*</sup> and Ana Asenjo-Garcia<sup>1,†</sup>

<sup>1</sup>*Department of Physics, Columbia University, New York, NY 10027, USA*

(Dated: March 23, 2022)

Dicke superradiance, where a decaying ensemble of atoms synchronizes to emit a short intense pulse of light, was one of the first described many-body collective effects in quantum optics. While well understood in cavities or in extremely small ensembles, superradiance remains an open problem in systems of size well beyond the atomic transition wavelength. Here we show that superradiance is a universal phenomenon in ordered arrays, and will generically occur if the inter-atomic distance is small enough. We also derive a concise expression – which is applicable to arrays of any dimensionality and topology – that allows us to predict the critical distance beyond which superradiance disappears. While correlated decay is a quantum many-body phenomenon that involves an exponentially large number of degrees of freedom, this expression only grows linearly with atom number, enabling us to study very large systems. Our predictions can be tested in state of the art experiments with arrays of neutral atoms, molecules, or even solid state emitters and pave the way towards understanding the role of collective emission in quantum simulation, metrology, and lasing.

As first discussed by Dicke, atoms placed in close proximity alter each others' radiative environment and emit light collectively [1–4]. The “environment” for each of the atoms depends on the internal state of all others, which changes in time, fundamentally altering the form of decay. In the highly-symmetric case of fully-inverted atoms at a single spatial location, correlated decay translates into the emission of a short pulse of light that initially rises in intensity, in contrast to the exponential decay of independent atoms. This “superradiant burst” occurs because atoms synchronize as they decay, locking in phase and emitting at an increasing rate. Superradiant bursts have been observed in dense thermal gases [5–9], where short interparticle distances can lead to ringing in the tail of the burst. Superradiance has also been observed in cavity setups [10, 11], where the condition of atoms at a point is emulated by the confinement of the field to zero dimensions.

The survival of the superradiant burst in extended geometries remains mostly unsolved. From a theoretical point of view, the exponential growth of the Hilbert space prevents the realization of numerical simulations beyond a few atoms. Atoms at the same point are indistinguishable from each other, and can only occupy states that obey a particle-exchange symmetry, restricting the Hilbert space to  $N + 1$  completely symmetric states, where  $N$  is the atom number. However, in extended systems this symmetry is broken and evolution requires a Hilbert space which grows as  $2^N$ . Hence, studies of superradiant emission have been limited to small numbers of atoms [12, 13] or small numbers of excitations [14].

The recent experimental demonstrations of ordered atomic arrays, via optical tweezers [15–20] and optical lattices [21–24], demand a new outlook on the problem. The current experimental capabilities open a new world of possibilities, where hundreds of atoms can be placed almost in arbitrary positions. These setups can serve as

experimental test beds of superradiance in large systems.

Here, we find that superradiant decay generically arises even for extended systems of size much larger than the transition wavelength, as long as the inter-atomic distance is small enough. As the distance increases, there is a smooth crossover between a superradiant and a monotonically decreasing emission rate, as shown in Fig. 1. We obtain an analytical condition for superradiance, which is universal and provides a bound on the inter-atomic separation (which depends on the dimensionality of the array). Below this critical distance, signatures of superradiance may be seen in the emitted pulse. We circumvent the exponential scaling of the problem by noting that the nature of the decay can be deduced from the statistics of the first two emitted photons. This exponentially

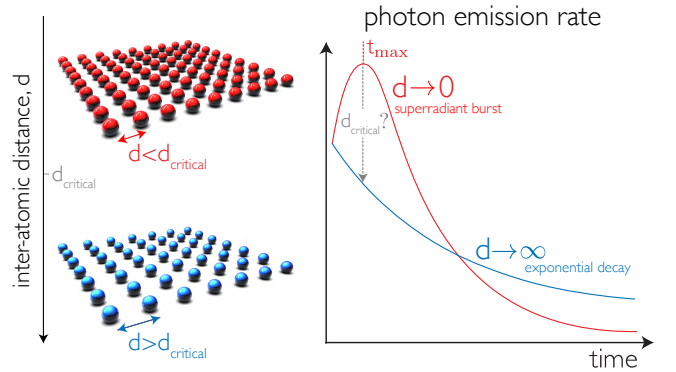


FIG. 1. Inverted atoms placed at the same location ( $d \rightarrow 0$ ) interact with each other and decay collectively via the emission of a burst of light, with a peak at time  $t_{\max}$ . This is the hallmark of Dicke superradiance. In contrast, atoms that are far separated ( $d \rightarrow \infty$ ) emit as a single atom would, in the form of an exponentially decaying pulse. For extended arrays, there is a critical distance at which the crossover between superradiance and monotonically decreasing emission occurs.

reduces the complexity, providing a tool to make predictions for very large atom numbers. We use this to study the role of geometry in the decay of finite-sized atomic arrays, providing a significant advance on a decades-old problem.

We first introduce the theoretical framework to deal with a collection of atoms interacting via a shared electromagnetic reservoir. We consider  $N$  two-level atoms of resonance frequency  $\omega_0$  and spontaneous emission rate  $\Gamma_0$  placed in arbitrary positions. After tracing out the reservoir degrees of freedom using a Born-Markov approximation [25, 26], the atomic density matrix  $\rho$  evolves according to

$$\dot{\rho} = -\frac{i}{\hbar}[\mathcal{H}, \rho] + \sum_{\nu=1}^N \frac{\Gamma_{\nu}}{2} \left( 2\hat{\mathcal{O}}_{\nu}\rho\hat{\mathcal{O}}_{\nu}^{\dagger} - \rho\hat{\mathcal{O}}_{\nu}^{\dagger}\hat{\mathcal{O}}_{\nu} - \hat{\mathcal{O}}_{\nu}^{\dagger}\hat{\mathcal{O}}_{\nu}\rho \right), \quad (1)$$

where  $\{\hat{\mathcal{O}}_{\nu}\}$  are the set of collective jump operators that represent photon emission and  $\{\Gamma_{\nu}\}$  their respective decay rates. In the above equation, the Hamiltonian is given by

$$\mathcal{H} = \hbar \sum_{i=1}^N \omega_0 \hat{\sigma}_{ee}^i + \hbar \sum_{i,j=1}^N J^{ij} \hat{\sigma}_{eg}^i \hat{\sigma}_{ge}^j, \quad (2)$$

where  $\hat{\sigma}_{ge}^i = |g_i\rangle\langle e_i|$  is the atomic coherence operator,  $|e_i\rangle$  and  $|g_i\rangle$  are the excited and ground states of the  $i$ th atom. The coherent and dissipative interaction rates between atoms  $i$  and  $j$  read [12, 27]

$$J^{ij} - i\frac{\Gamma^{ij}}{2} = -\frac{\mu_0\omega_0^2}{\hbar} \boldsymbol{\wp}^* \cdot \mathbf{G}_0(\mathbf{r}_i, \mathbf{r}_j, \omega_0) \cdot \boldsymbol{\wp}, \quad (3)$$

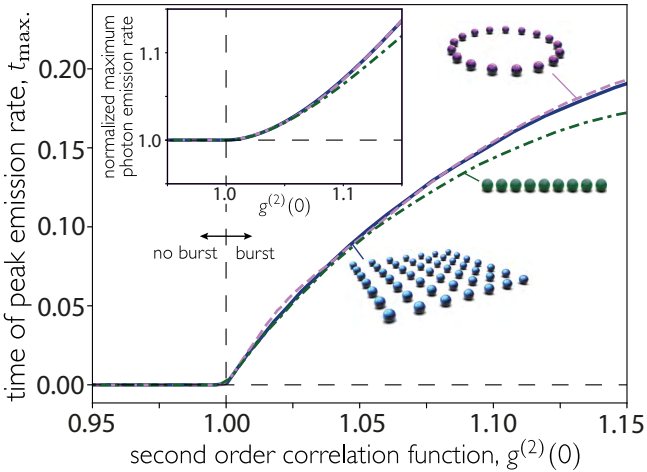


FIG. 2. We use photon statistics (at  $t = 0$ ) to predict superradiance, as an enhanced two-photon emission rate is a prerequisite for a burst. The time at which the photon rate is maximum ( $t_{\max}$ ) as a function of the second order correlation function (at  $t = 0$ ) shows that  $t_{\max} > 0$  only if  $g^{(2)}(0) > 1$ . Inset: Maximum intensity, normalized by intensity at  $t = 0$ . In both plots, all 9 atoms are initially excited, with polarization perpendicular to the array.

where  $\boldsymbol{\wp}$  is the dipole matrix element of the atomic transition and  $\mathbf{G}_0(\mathbf{r}_i, \mathbf{r}_j, \omega_0)$  is the propagator of the electromagnetic field (in vacuum) between atomic positions  $\mathbf{r}_i$  and  $\mathbf{r}_j$  [25, 26].

The atoms decay collectively due to dissipative interactions that occur as photons are emitted. As shown in Eq. (1), the dissipative part of the evolution can be diagonalized into  $N$  jump operators,  $\{\hat{\mathcal{O}}_{\nu}\}$ , found as the eigenstates of the dissipative interaction matrix  $\Gamma$  with elements  $\Gamma^{ij}$  [12, 27]. The corresponding eigenvalues provide the jump operator rates  $\{\Gamma_{\nu}\}$ , which represent how frequently such a jump occurs. The emission of a photon lowers the number of excitations by one. Therefore, the action of a jump operator on the ensemble corresponds to the action of a superposition of atomic lowering operators  $\hat{\mathcal{O}}_{\nu} = \sum_{i=1}^N \alpha_{\nu,i} \hat{\sigma}_{ge}^i$ , where  $\alpha_{\nu,i}$  represents some spatial profile.

In the paradigmatic example of Dicke superradiance, where all atoms are exactly at one point, only one of the jump operators is bright (with decay rate  $\Gamma_{\nu} = N\Gamma_0$ ), while all the others are completely dark (i.e., their rate of action is exactly zero). This means that the only possible decay path to the ground state for atoms that are initially excited is through repeated action of the (symmetric) bright operator, which imprints a phase pattern in the atoms that is reinforced in each process of photon emission. Coherence thus emerges via this dissipative mechanism, which leads to the development of a macroscopic dipole through synchronization and to a rapid release of energy in the form of a superradiant burst, whose peak intensity scales as  $N^2$  [1].

In contrast, in ordered arrays, all jump operators are allowed to act and their decay rates vary dramatically due to constructive and destructive interference. They can be larger (bright) or smaller (dark) than the single atom decay rate  $\Gamma_0$ . Extremely dark rates, which are strictly zero in the thermodynamic limit, emerge for inter-atomic separations below a certain distance that depends on the dimensionality of the array. For 1D arrays, such distance is  $d < \lambda_0/2$  (with  $\lambda_0$  being the atomic transition wavelength); for 2D arrays, the distance is  $d < \lambda_0$ ; and for 3D arrays it is even larger [28].

We show here that superradiance generically occurs in arrays, but only below a critical inter-atomic distance. Dissipative interactions, rather than the coherent Hamiltonian dynamics, are to blame for the suppression of superradiance [12, 13]. As the distance grows, the decay rate distribution of the different jump operators becomes more uniform. This leads to a strong competition between them, and to decoherence through the randomization of the atomic phases after several emission processes have occurred. The superradiant burst diminishes as the inter-atomic distance increases, eventually being replaced by a monotonically decaying pulse. The crossover between these regimes is marked by an infinitesimally small burst that occurs at  $t = 0$  [13]. Atomic synchronization

occurs immediately or not at all, such that the nature of the decay can be characterized from early dynamics.

Our key insight is that one can predict the nature of the decay based solely on the statistics of the first two emitted photons. The minimum requirement for a superradiant burst to occur is that the first photon enhances the emission rate of the second. This is captured by the second order correlation function

$$g^{(2)}(0) = \frac{\sum_{\nu,\mu=1}^N \Gamma_\nu \Gamma_\mu \langle \hat{G}_\nu^\dagger \hat{G}_\mu^\dagger \hat{G}_\mu \hat{G}_\nu \rangle}{\left( \sum_{\nu=1}^N \Gamma_\nu \langle \hat{G}_\nu^\dagger \hat{G}_\nu \rangle \right)^2}, \quad (4)$$

where the expectation value is taken at the initial state, i.e.,  $|\psi(t=0)\rangle = |e\rangle^{\otimes N}$ . When this quantity is greater than unity, the decay is characterized as superradiant. Figure 2 shows the correlation between  $g^{(2)}(0)$  and the presence or absence of a burst for small atom numbers, for which we can calculate the full dynamics. As soon as  $g^{(2)}(0) > 1$ , the time of maximum emission deviates from zero (i.e., the burst emerges at a finite time). Moreover, the second order correlation function increases along with the height of the peak of the photon emission rate, and is below unity when the rate is peaked at  $t = 0$  (i.e., when there is no superradiance).

The second order correlation function  $g^{(2)}(0)$  can be calculated analytically (see Appendix A), and we thus obtain the minimal condition for superradiance, which reads

$$g^{(2)}(0) = 1 + \frac{1}{N} \left[ \text{Var} \left( \frac{\{\Gamma_\nu\}}{\Gamma_0} \right) - 1 \right] > 1, \quad (5)$$

where Var is the variance of the decay rates of the jump operators. It can be re-written as

$$\text{Var} \left( \frac{\{\Gamma_\nu\}}{\Gamma_0} \right) > 1. \quad (6)$$

This expression is exact and universal: it makes no assumptions about the atomic positions, beyond that exchange interactions are symmetric (which is true in free space and in any reciprocal medium). Small inter-atomic distances maximize the variance of the eigenvalues, as most of them will be dark and just a small number of them will be bright.

We note that the complexity of the problem has decreased tremendously: from solving a differential equation in an exponentially-growing Hilbert space, to diagonalizing a matrix whose dimension scales linearly with atom number. This allows one to find the distance at which superradiance disappears in arbitrary geometries with an extremely large atom number, as all the details about dimensionality and polarization are captured in the dissipative interaction matrix  $\Gamma$ . Of course, one has to pay a price for this reduction in complexity. As we

cannot calculate the full evolution, we can only predict whether superradiance is going to occur or not, not the height of the peak nor the time at which it will appear.

In order to use the above inequalities to characterize superradiance, we demonstrate that the system does not rephase at later times, either through further dissipation or through Hamiltonian action. First, we show the impact of coherent interactions by switching on and off the Hamiltonian, as shown in Fig. 3(a). At early times, dissipation dominates and the Hamiltonian does not significantly impact the dynamics. We also investigate whether the Hamiltonian rephases the system by considering a time delay  $\tau$  between the emission of two photons, during which the Hamiltonian acts. In this case, the Hamil-

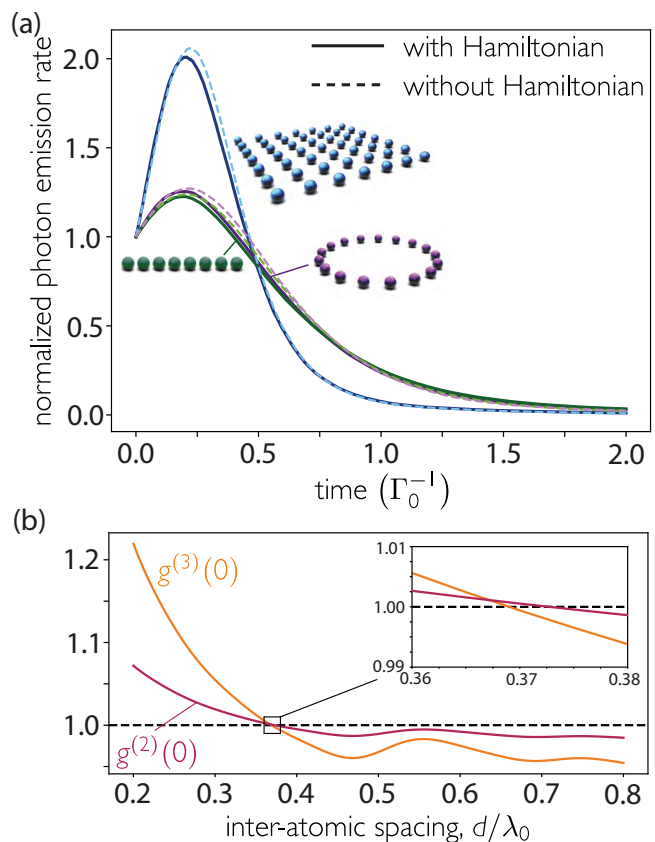


FIG. 3. Role of dissipative and coherent evolution in dephasing and suppression of superradiance. (a) The coherent evolution does not significantly modify the early time dynamics, thus preserving superradiance, as shown by the full evolution of the master equation [i.e., Eq. (1)] for 16 initially excited atoms with inter-atomic distance  $d = 0.1\lambda_0$  arranged in different geometries with and without Hamiltonian interactions. Emission rate is normalized by that at  $t = 0$ . (b) Three-photon decay is never enhanced unless two-photon emission is too, as demonstrated by the second and third order correlation functions, plotted as a function of the inter-atomic separation for a square 2D array of  $6 \times 6$  atoms. In all cases, atoms are polarized perpendicular to the array.

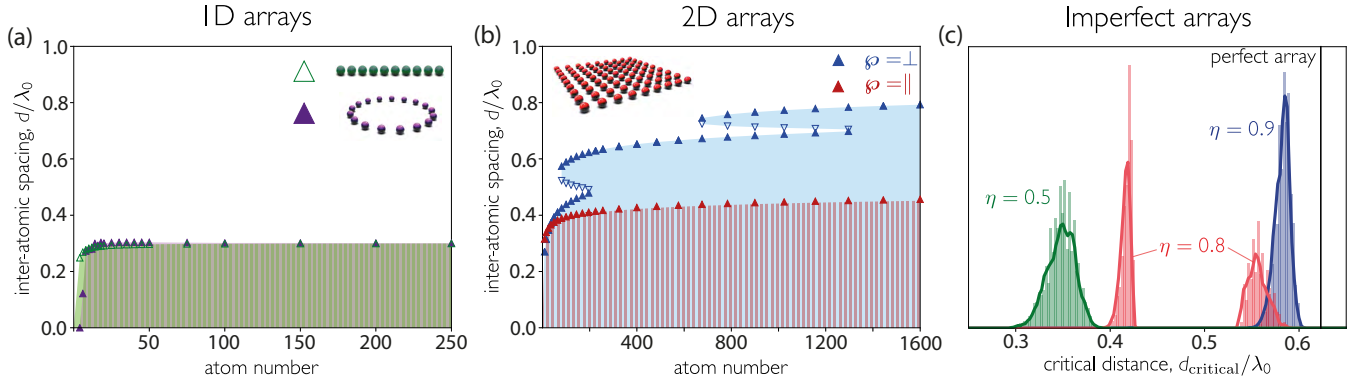


FIG. 4. Superradiance is universal and appears (below a critical distance) for arrays of any dimensionality, including imperfectly-filled ones. (a,b) Boundaries between the burst (colored) and no-burst (white) regions as a function of inter-atomic distance  $d$  and atom number for (a) chains and rings and (b) square arrays. The crossover occurs where  $g^{(2)}(0) = 1$ . The symbols  $\triangle$  and  $\nabla$  represent points where, with decreasing  $d$ ,  $g^{(2)}(0)$  goes above and below unity, respectively. (c) Critical distance for different filling fractions  $\eta$ . The histogram shows 2000 configurations of a  $12 \times 12$  site square arrays stochastically filled with efficiency  $\eta$ . Envelopes are calculated as rolling averages. Atoms are polarized (a) parallel to the array (for the ring this implies a spatially-dependent polarization), (b) perpendicular (blue) and parallel (red) to the plane, and (c) perpendicular to the plane.

tonian adds a slow dephasing to the atoms but, importantly, it does not enhance photon emission. This has long been known to be the case for all atomic geometries without atom-exchange symmetry [3, 4, 29]. Second, we characterize the impact of further jumps through higher-order correlation functions. The third order correlation function can be analytically calculated (see Appendix B). For all geometries here considered, the third photon is never enhanced when the second photon is not. Therefore, further jumps do not rephase the array, as shown in Fig. 3(b), where  $g^{(3)}(0)$  drops below unity at a slightly smaller distance than  $g^{(2)}(0)$ . As anticipated, the second photon is the last one to lose its stimulated enhancement.

We can now investigate superradiance in very large arrays of different dimensionality and topology. Contrary to the accepted understanding in the literature [3, 4], we find that large chains and rings behave almost identically, as both lose superradiance at  $d_{\text{critical}} \approx 0.3\lambda_0$ , as shown in Fig. 3(a). Despite the ring’s atom-exchange symmetry, the difference between the ring and the chain is negligible for large atom number. This is in line with the understanding that dephasing is caused by competition between multiple decay channels, which exist regardless of the topology [13]. Interactions across the diameter of the ring are very weak, so the exchange symmetry does not matter, as the atoms essentially see the same local environment in both cases.

Two- and three-dimensional arrays also display superradiance, at larger inter-atomic separations than those found in chains. Interestingly, the total size of the array is much larger than a wavelength. Figure 3(b) shows the critical distance for a 2D square array of up to  $40 \times 40$  atoms. In this geometry, the critical distance is not monotonic with the atom number. These sudden vari-

ations are due to “revivals” in  $g^{(2)}(0)$ , which can be seen in Fig. 3(b), associated with changes in the distribution of  $\{\Gamma_\nu\}$  as the lattice constant hits certain geometric resonances [30–33]. For large arrays, the critical distance is as large as  $d_{\text{critical}} \approx 0.8\lambda_0$  for atoms polarized perpendicular to the array surface.

The survival of superradiance at large inter-atomic distances is due to the presence of dark operators. The sum of the jump operator decay rates is always  $N\Gamma_0$ , regardless of the atomic positions. The bright operators required for superradiance must be balanced by dark operators. In ordered arrays, the presence of extremely dark operators is explained by energy-momentum mismatch, with dark operators defined as spin waves with wave-vectors outside the light cone [28, 34]. In 2D arrays, the operator that acts with equal phase on all sites, corresponding to a wave-vector  $\{k_x = 0, k_y = 0\}$ , has no momentum in the plane and emits perpendicular to the array. If the atomic dipole axis points in that direction then emission is forbidden, creating a region of subradiance that persists to  $d < \lambda_0$  [28]. This explains why the crossover between superradiant decay to monotonic decay occurs at much larger distances for 2D arrays with this polarization. The same phenomenon exists in 3D lattices for any linear polarization axis, with preliminary calculations showing values for the critical distance beyond  $\lambda_0$ .

We also demonstrate that superradiance is robust to experimental imperfections typically found in experiments, such as filling fraction smaller than unity. Figure 4(c) shows the bound for stochastically generated  $12 \times 12$  arrays filled with efficiency  $\eta$ . For  $\eta = 90\%$ , there is a small reduction in the critical distance. However, at  $\eta = 50\%$ , the drop is much larger. This is because the



revivals in  $g^{(2)}(0)$  are particularly muted by imperfect filling, and at this efficiency do not breach unity. This phenomenon is also responsible for the splitting of the values of  $d_{\text{critical}}$  at 80% filling efficiency. Experimentally, one can counteract a low filling fraction by working with arrays of small lattice constants.

Dicke superradiance should thus be observable in experiments with arrays of inter-atomic separation below the critical distance, which are close to being achieved in state-of-the-art setups [35, 36]. It is important to notice that the critical distance does not signal a sharp transition between monotonic decay and superradiance, but instead a smooth crossover. Experiments should thus aim to be well below this bound. Besides atomic tweezer arrays and optical lattices, solid-state emitters hosted in bulk crystals [37, 38] or in 2D materials [39–41] are good candidates to observe this physics. These systems can achieve small lattice constants, although they present other difficulties such as inhomogeneous broadening and non-radiative decay rate. Nevertheless, these (as well as a modification of the propagator due to the change of dielectric environment) can be included in the theoretical treatment, which will be done in future work.

Superradiance in an extended array is very different from superradiance in a cavity. In the latter, superradiance involves three phenomena simultaneously: a growth in the photon emission rate, a rapid increase of the population of the cavity mode (due to the burst), and an  $N^2$ -scaling of the radiated intensity peak. These three concepts are not equivalent for extended arrays in free space, and this has experimental consequences. First, in free space, photons are scattered in all directions, and the relevant geometry is not only that of the array, but that of the array together with the detector. In this work, we effectively integrate over all directions, which would correspond to collecting light over a large solid angle. As photon emission after a jump is directional [12, 13], the burst is most optimally measured by a detector placed at the location where the far field distribution of the brightest jump operator is maximal. Slightly below and above the critical distance, a burst in the integrated photon emission rate does not necessarily correspond to a burst in the intensity radiated in a certain direction. Second, the peak intensity may no longer scale as  $N^2$ . Finding the exact scaling theoretically is extremely challenging as it requires full dynamical evolution, though it should be accessible in experiments.

In conclusion, we have demonstrated that many-body superradiance universally appears in atomic arrays with small lattice constant, but with total extension well beyond the resonance wavelength. We have also bounded the critical distance that signals the crossover between monotonic decay and a superradiant burst. This bound is found by diagonalizing a matrix that scales only linearly with atom number. This method bypasses the exponentially growing Hilbert space required for full evolution

by simplifying the problem to the statistics of the first two photons, which allows us to predict superradiance for very large arrays. Our approach may be extended to disordered atomic ensembles [42, 43] (where very small inter-atomic distances are achievable), to other types of electromagnetic reservoirs, such as nanophotonic structures (by simply changing the Green’s function [44–47]), and to emitters with a more complex internal or hyper-fine structure [48–50].

Beyond advancing fundamental science, understanding many-body decay is critical for developing robust quantum applications, ranging from quantum computing and simulation to metrology and lasing. In particular, our work is relevant for Rydberg atom quantum simulators [51–57], where Rydberg states may decay via long-wavelength transitions. These decay paths may be superradiantly enhanced at short distances [58, 59]. Atomic arrays are also used in state-of-the-art atomic clocks and other precision measurement experiments [60, 61]. As such systems shrink, it is crucial to understand the impact of collective dissipation. Finally, controlling the light emitted by an atomic array enables its use as an optical source. We have demonstrated that geometry can be used to alter the collective optical properties of the array and shape the temporal profile and statistics of the emitted light. This presents the opportunity to use atomic arrays to produce directional single photons [62], correlated photons [13], or superradiant lasers [63]. Alternatively, measurement of the emitted light provides a window into the complex evolution of the atomic system; and directional detection may enable heralded production of many-body entangled dark states.

**Acknowledgments** – We are grateful to L. A. Orozco, I. Ferrier-Barbut, A. Browaeys, D. E. Chang, and E. Sierra for stimulating discussions. Research was supported by Programmable Quantum Materials, an Energy Frontier Research Center funded by the U.S. Department of Energy (DOE), Office of Science, Basic Energy Sciences (BES).

---

\* s.j.masson@columbia.edu

† ana.asenjo@columbia.edu

- [1] R. H. Dicke, Coherence in spontaneous radiation processes, *Phys. Rev.* **93**, 99 (1954).
- [2] N. E. Rehler and J. H. Eberly, Superradiance, *Phys. Rev. A* **3**, 1735 (1971).
- [3] M. Gross and S. Haroche, Superradiance: An essay on the theory of collective spontaneous emission, *Phys. Rep.* **93**, 301 (1982).
- [4] M. G. Benedict, A. M. Ermolaev, V. A. Malyshev, I. V. Sokolov, and E. D. Trifonov, *Super-radiance: Multiatomic Coherent Emission* (CRC Press, 1996).
- [5] N. Skribanowitz, I. P. Herman, J. C. MacGillivray, and M. S. Feld, Observation of Dicke superradiance in optically pumped HF gas, *Phys. Rev. Lett.* **30**, 309 (1973).

- [6] M. Gross, C. Fabre, P. Pillet, and S. Haroche, Observation of near-infrared Dicke superradiance on cascading transitions in atomic sodium, *Phys. Rev. Lett.* **36**, 1035 (1976).
- [7] A. Flusberg, T. Mossberg, and S. R. Hartmann, Optical difference-frequency generation in atomic thallium vapor, *Phys. Rev. Lett.* **38**, 59 (1977).
- [8] S. Inouye, A. P. Chikkatur, D. M. Stamper-Kurn, J. Stenger, D. E. Pritchard, and W. Ketterle, Superradiant Rayleigh scattering from a Bose-Einstein condensate, *Science* **285**, 571 (1999).
- [9] M. Scheibner, T. Schmidt, L. Worschech, A. Forchel, G. Bacher, T. Passow, and D. Hommel, Superradiance of quantum dots, *Nature Physics* **3**, 106 (2007).
- [10] J. M. Raimond, P. Goy, M. Gross, C. Fabre, and S. Haroche, Collective absorption of blackbody radiation by Rydberg atoms in a cavity: An experiment on Bose statistics and Brownian motion, *Phys. Rev. Lett.* **49**, 117 (1982).
- [11] S. Slama, S. Bux, G. Krenz, C. Zimmermann, and P. W. Courteille, Superradiant Rayleigh scattering and collective atomic recoil lasing in a ring cavity, *Phys. Rev. Lett.* **98**, 053603 (2007).
- [12] J. P. Clemens, L. Horvath, B. C. Sanders, and H. J. Carmichael, Collective spontaneous emission from a line of atoms, *Phys. Rev. A* **68**, 023809 (2003).
- [13] S. J. Masson, I. Ferrier-Barbut, L. A. Orozco, A. Browaeys, and A. Asenjo-Garcia, Many-body signatures of collective decay in atomic chains, *Phys. Rev. Lett.* **125**, 263601 (2020).
- [14] M. O. Scully, E. S. Fry, C. H. Raymond Ooi, and K. Wódkiewicz, Directed spontaneous emission from an extended ensemble of  $n$  atoms: Timing is everything, *Phys. Rev. Lett.* **96**, 010501 (2006).
- [15] H. Kim, W. Lee, H.-G. Lee, H. Jo, Y. Song, and J. Ahn, In situ single-atom array synthesis using dynamic holographic optical tweezers, *Nat. Commun.* **7**, 13317 (2016).
- [16] M. Endres, H. Bernien, A. Keesling, H. Levine, E. R. Anschuetz, A. Krajenbrink, C. Senko, V. Vuletic, M. Greiner, and M. D. Lukin, Atom-by-atom assembly of defect-free one-dimensional cold atom arrays, *Science* **354**, 1024 (2016).
- [17] D. Barredo, S. de Léséleuc, V. Lienhard, T. Lahaye, and A. Browaeys, An atom-by-atom assembler of defect-free arbitrary two-dimensional atomic arrays, *Science* **354**, 1021 (2016).
- [18] M. A. Norcia, A. W. Young, and A. M. Kaufman, Microscopic control and detection of ultracold strontium in optical-tweezer arrays, *Phys. Rev. X* **8**, 041054 (2018).
- [19] S. Saskin, J. T. Wilson, B. Grinkemeyer, and J. D. Thompson, Narrow-line cooling and imaging of ytterbium atoms in an optical tweezer array, *Phys. Rev. Lett.* **122**, 143002 (2019).
- [20] D. Ohl de Mello, D. Schäffner, J. Werkmann, T. Preuschoff, L. Kohfahl, M. Schlosser, and G. Birkel, Defect-free assembly of 2D clusters of more than 100 single-atom quantum systems, *Phys. Rev. Lett.* **122**, 203601 (2019).
- [21] W. S. Bakr, A. Peng, M. E. Tai, R. Ma, J. Simon, J. I. Gillen, S. Fölling, L. Pollet, and M. Greiner, Probing the superfluid-to-Mott insulator transition at the single-atom level, *Science* **329**, 547 (2010).
- [22] J. F. Sherson, C. Weitenberg, M. Endres, M. Cheneau, I. Bloch, and S. Kuhr, Single-atom-resolved fluorescence imaging of an atomic Mott insulator, *Nature* **467**, 68 (2010).
- [23] D. Greif, M. F. Parsons, A. Mazurenko, C. S. Chiu, S. Blatt, F. Huber, G. Ji, and M. Greiner, Site-resolved imaging of a fermionic Mott insulator, *Science* **351**, 953 (2016).
- [24] A. Kumar, T.-Y. Wu, F. Giraldo, and D. S. Weiss, Sorting ultracold atoms in a three-dimensional optical lattice in a realization of Maxwell's demon, *Nature* **561**, 83 (2018).
- [25] T. Gruner and D.-G. Welsch, Green-function approach to the radiation-field quantization for homogeneous and inhomogeneous Kramers-Kronig dielectrics, *Phys. Rev. A* **53**, 1818 (1996).
- [26] H. T. Dung, L. Knöll, and D.-G. Welsch, Resonant dipole-dipole interaction in the presence of dispersing and absorbing surroundings, *Phys. Rev. A* **66**, 063810 (2002).
- [27] H. J. Carmichael and K. Kim, A quantum trajectory unraveling of the superradiance master equation, *Opt. Commun.* **179**, 417 (2000).
- [28] A. Asenjo-Garcia, M. Moreno-Cardoner, A. Albrecht, H. J. Kimble, and D. E. Chang, Exponential improvement in photon storage fidelities using subradiance and "selective radiance" in atomic arrays, *Phys. Rev. X* **7**, 031024 (2017).
- [29] R. Friedberg and S. R. Hartmann, Superradiant stability in specially shaped small samples, *Opt. Commun.* **10**, 298 (1974).
- [30] R. J. Bettles, S. A. Gardiner, and C. S. Adams, Cooperative ordering in lattices of interacting two-level dipoles, *Phys. Rev. A* **92**, 063822 (2015).
- [31] R. J. Bettles, S. A. Gardiner, and C. S. Adams, Enhanced optical cross section via collective coupling of atomic dipoles in a 2D array, *Phys. Rev. Lett.* **116**, 103602 (2016).
- [32] S. Krämer, L. Ostermann, and H. Ritsch, Optimized geometries for future generation optical lattice clocks, *EPL (Europhysics Letters)* **114**, 14003 (2016).
- [33] J. Javanainen and R. Rajapakse, Light propagation in systems involving two-dimensional atomic lattices, *Phys. Rev. A* **100**, 013616 (2019).
- [34] H. Zoubi and H. Ritsch, Metastability and directional emission characteristics of excitons in 1D optical lattices, *Europhys. Lett.* **90**, 23001 (2010).
- [35] J. Rui, D. Wei, A. Rubio-Abadal, S. Hollerith, J. Zeiher, D. M. Stamper-Kurn, C. Gross, and I. Bloch, A subradiant optical mirror formed by a single structured atomic layer, *Nature* **583**, 369 (2020).
- [36] A. Glicenstein, G. Ferioli, N. Šibalić, L. Brossard, I. Ferrier-Barbut, and A. Browaeys, Collective shift in resonant light scattering by a one-dimensional atomic chain, *Phys. Rev. Lett.* **124**, 253602 (2020).
- [37] T. Kornher, K. Xia, R. Kolesov, N. Kukharchyk, R. Reuter, P. Siyushev, R. Stöhr, M. Schreck, H.-W. Becker, B. Villa, A. D. Wieck, and J. Wrachtrup, Production yield of rare-earth ions implanted into an optical crystal, *Appl. Phys. Lett.* **108**, 053108 (2016).
- [38] A. Sipahigil, R. E. Evans, D. D. Sukachev, M. J. Burek, J. Borregaard, M. K. Bhaskar, C. T. Nguyen, J. L. Pacheco, H. A. Atikian, C. Meuwly, R. M. Camacho, F. Jelezko, E. Bielejec, H. Park, M. Lončar, and M. D. Lukin, An integrated diamond nanophotonics platform for quantum-optical networks, *Science* **354**, 847 (2016).
- [39] C. Palacios-Berraquero, D. M. Kara, A. R. P. Mont-

- blanch, M. Barbone, P. Latawiec, D. Yoon, A. K. Ott, M. Loncar, A. C. Ferrari, and M. Atatüre, Large-scale quantum-emitter arrays in atomically thin semiconductors, *Nat. Commun.* **8**, 15093 (2017).
- [40] N. V. Proscia, Z. Shotan, H. Jayakumar, P. Reddy, C. Cohen, M. Dollar, A. Alkauskas, M. Doherty, C. A. Meriles, and V. M. Menon, Near-deterministic activation of room-temperature quantum emitters in hexagonal boron nitride, *Optica* **5**, 1128 (2018).
- [41] C. Li, N. Mendelson, R. Ritika, Y. Chen, Z.-Q. Xu, M. Toth, and I. Aharonovich, Scalable and deterministic fabrication of quantum emitter arrays from hexagonal boron nitride, *Nano Lett.* **21**, 3626 (2021).
- [42] W. Guerin, M. O. Araújo, and R. Kaiser, Subradiance in a large cloud of cold atoms, *Phys. Rev. Lett.* **116**, 083601 (2016).
- [43] G. Ferioli, A. Glicenstein, L. Henriët, I. Ferrier-Barbut, and A. Browaeys, Storage and release of subradiant excitations in a dense atomic cloud, *Phys. Rev. X* **11**, 021031 (2021).
- [44] D. E. Chang, J. I. Cirac, and H. J. Kimble, Self-organization of atoms along a nanophotonic waveguide, *Phys. Rev. Lett.* **110**, 113606 (2013).
- [45] A. Asenjo-Garcia, J. D. Hood, D. E. Chang, and H. J. Kimble, Atom-light interactions in quasi-one-dimensional nanostructures: A Green's-function perspective, *Phys. Rev. A* **95**, 033818 (2017).
- [46] P. Solano, P. Barberis-Blostein, F. K. Fatemi, L. A. Orozco, and S. L. Rolston, Super-radiance reveals infinite-range dipole interactions through a nanofiber, *Nat. Commun.* **8**, 1857 (2017).
- [47] D. E. Chang, J. S. Douglas, A. González-Tudela, C.-L. Hung, and H. J. Kimble, Colloquium: Quantum matter built from nanoscopic lattices of atoms and photons, *Rev. Mod. Phys.* **90**, 031002 (2018).
- [48] M. Hebenstreit, B. Kraus, L. Ostermann, and H. Ritsch, Subradiance via entanglement in atoms with several independent decay channels, *Phys. Rev. Lett.* **118**, 143602 (2017).
- [49] A. Asenjo-Garcia, H. J. Kimble, and D. E. Chang, Optical waveguiding by atomic entanglement in multilevel atom arrays, *Proc. Natl. Acad. Sci. USA* **116**, 25503 (2019).
- [50] A. Piñeiro Orioli, J. K. Thompson, and A. M. Rey, Emergent dark states from superradiant dynamics in multi-level atoms in a cavity, *arXiv:2106.00019* (2021).
- [51] H. Labuhn, D. Barredo, S. Ravets, S. de Léséleuc, T. Macrì, T. Lahaye, and A. Browaeys, Tunable two-dimensional arrays of single Rydberg atoms for realizing quantum Ising models, *Nature* **534**, 667 (2016).
- [52] H. Bernien, S. Schwartz, A. Keesling, H. Levine, A. Omran, H. Pichler, S. Choi, A. S. Zibrov, M. Endres, M. Greiner, V. Vuletić, and M. D. Lukin, Probing many-body dynamics on a 51-atom quantum simulator, *Nature* **551**, 579 (2017).
- [53] H. Kim, Y.-J. Park, K. Kim, H.-S. Sim, and J. Ahn, Detailed balance of thermalization dynamics in Rydberg-atom quantum simulators, *Phys. Rev. Lett.* **120**, 180502 (2018).
- [54] A. Keesling, A. Omran, H. Levine, H. Bernien, H. Pichler, S. Choi, R. Samajdar, S. Schwartz, P. Silvi, S. Sachdev, P. Zoller, M. Endres, M. Greiner, V. Vuletić, and M. D. Lukin, Quantum Kibble-Zurek mechanism and critical dynamics on a programmable Rydberg simulator, *Nature* **568**, 207 (2019).
- [55] S. de Léséleuc, V. Lienhard, P. Scholl, D. Barredo, S. Weber, N. Lang, H. P. Büchler, T. Lahaye, and A. Browaeys, Observation of a symmetry-protected topological phase of interacting bosons with Rydberg atoms, *Science* **365**, 775 (2019).
- [56] D. Bluvstein, A. Omran, H. Levine, A. Keesling, G. Semeghini, S. Ebadi, T. T. Wang, A. A. Michailidis, N. Maskara, W. W. Ho, S. Choi, M. Serbyn, M. Greiner, V. Vuletić, and M. D. Lukin, Controlling quantum many-body dynamics in driven Rydberg atom arrays, *Science* **371**, 1355 (2021).
- [57] S. Ebadi, T. T. Wang, H. Levine, A. Keesling, G. Semeghini, A. Omran, D. Bluvstein, R. Samajdar, W. W. Pichler, Hannes an Ho, S. Choi, S. Sachdev, M. Greiner, V. Vuletic, and M. D. Lukin, Quantum phases of matter on a 256-atom programmable quantum simulator, *arXiv:2012.12281* (2020).
- [58] T. Wang, S. F. Yelin, R. Côté, E. E. Eyler, S. M. Farooqi, P. L. Gould, M. Koštrun, D. Tong, and D. Vranceanu, Superradiance in ultracold Rydberg gases, *Phys. Rev. A* **75**, 033802 (2007).
- [59] E. A. Goldschmidt, T. Boulier, R. C. Brown, S. B. Koller, J. T. Young, A. V. Gorshkov, S. L. Rolston, and J. V. Porto, Anomalous broadening in driven dissipative Rydberg systems, *Phys. Rev. Lett.* **116**, 113001 (2016).
- [60] T. Bothwell, D. Kedar, E. Oelker, J. M. Robinson, S. L. Bromley, W. L. Tew, J. Ye, and C. J. Kennedy, JILA SrI optical lattice clock with uncertainty of  $2.0 \times 10^{-18}$ , *Metrologia* **56**, 065004 (2019).
- [61] M. A. Norcia, A. W. Young, W. J. Eckner, E. Oelker, J. Ye, and A. M. Kaufman, Seconds-scale coherence on an optical clock transition in a tweezer array, *Science* **366**, 93 (2019).
- [62] R. Holzinger, M. Moreno-Cardoner, and H. Ritsch, Nanoscale continuous quantum light sources based on drive dipole emitter arrays, *arXiv:2103.02416* (2021).
- [63] J. G. Bohnet, Z. Chen, J. M. Weiner, D. Meiser, M. J. Holland, and J. K. Thompson, A steady-state superradiant laser with less than one intracavity photon, *Nature* **484**, 78 (2012).

# APPENDIX A: DERIVATION OF THE SECOND ORDER CORRELATION FUNCTION $g^{(2)}(0)$

We consider the second order correlation function, calculated as

$$g^{(2)}(0) = \frac{\sum_{\nu,\mu=1}^N \Gamma_\nu \Gamma_\mu \langle \hat{\sigma}_\nu^\dagger \hat{\sigma}_\mu^\dagger \hat{\sigma}_\mu \hat{\sigma}_\nu \rangle}{\left( \sum_{\nu=1}^N \Gamma_\nu \langle \hat{\sigma}_\nu^\dagger \hat{\sigma}_\nu \rangle \right)^2}, \quad (7)$$

where the expectation value is taken on the fully excited state  $|e\rangle^{\otimes N}$ , which is the initial state of the system. We can generically expand out the form of the jump operators

$$\hat{\sigma}_\nu = \sum_{i=1}^N \alpha_{\nu,i} \hat{\sigma}_{ge}^i, \quad \text{where} \quad \sum_{i=1}^N \alpha_{\nu,i}^* \alpha_{\mu,i} = \delta_{\nu\mu} \quad \text{and} \quad \sum_{\nu=1}^N \Gamma_\nu |\alpha_{\nu,i}|^2 = \Gamma_0. \quad (8)$$

In the above expression,  $\delta_{\mu\nu}$  is the Kronecker delta function. Substituting these equations into Eq. (7) one finds

$$g^{(2)}(0) = \frac{\sum_{\nu,\mu=1}^N \Gamma_\nu \Gamma_\mu \sum_{i,j,l,m=1}^N \alpha_{\nu,i}^* \alpha_{\mu,j}^* \alpha_{\mu,l} \alpha_{\nu,m} \langle \hat{\sigma}_{eg}^i \hat{\sigma}_{eg}^j \hat{\sigma}_{ge}^l \hat{\sigma}_{ge}^m \rangle}{\left( \sum_{\nu=1}^N \Gamma_\nu \sum_{i,j=1}^N \alpha_{\nu,i}^* \alpha_{\nu,j} \langle \hat{\sigma}_{eg}^i \hat{\sigma}_{ge}^j \rangle \right)^2}. \quad (9)$$

On the fully excited state, these expectation values are evaluated as

$$\langle \hat{\sigma}_{eg}^i \hat{\sigma}_{ge}^j \rangle = \delta_{ij}, \quad (10)$$

$$\langle \hat{\sigma}_{eg}^i \hat{\sigma}_{eg}^j \hat{\sigma}_{ge}^l \hat{\sigma}_{ge}^m \rangle = (\delta_{im} \delta_{jl} + \delta_{il} \delta_{jm}) (1 - \delta_{ij}). \quad (11)$$

Therefore,

$$\begin{aligned} g^{(2)}(0) &= \frac{\sum_{\nu,\mu=1}^N \Gamma_\nu \Gamma_\mu \sum_{i,j,l,m=1}^N \alpha_{\nu,i}^* \alpha_{\mu,j}^* \alpha_{\mu,l} \alpha_{\nu,m} (\delta_{im} \delta_{jl} + \delta_{il} \delta_{jm}) (1 - \delta_{ij})}{\left( \sum_{\nu=1}^N \Gamma_\nu \sum_{i,j=1}^N \alpha_{\nu,i}^* \alpha_{\nu,j} \delta_{ij} \right)^2} \\ &= \frac{\sum_{\nu,\mu=1}^N \Gamma_\nu \Gamma_\mu \left( \sum_{i,j=1}^N |\alpha_{\nu,i}|^2 |\alpha_{\mu,j}|^2 + \alpha_{\nu,i}^* \alpha_{\mu,j}^* \alpha_{\mu,i} \alpha_{\nu,j} - 2 \sum_{i=1}^N |\alpha_{\nu,i}|^2 |\alpha_{\mu,i}|^2 \right)}{\left( \sum_{\nu=1}^N \Gamma_\nu \sum_{i=1}^N |\alpha_{\nu,i}|^2 \right)^2} \\ &= \frac{\sum_{\nu,\mu=1}^N \Gamma_\nu \Gamma_\mu \left[ \left( \sum_{i=1}^N |\alpha_{\nu,i}|^2 \right) \left( \sum_{j=1}^N |\alpha_{\mu,j}|^2 \right) + \left( \sum_{i=1}^N \alpha_{\nu,i}^* \alpha_{\mu,i} \right) \left( \sum_{j=1}^N \alpha_{\mu,j}^* \alpha_{\nu,j} \right) - 2 \sum_{i=1}^N |\alpha_{\nu,i}|^2 |\alpha_{\mu,i}|^2 \right]}{N^2 \Gamma_0^2} \\ &= \frac{\sum_{\nu,\mu=1}^N \Gamma_\nu \Gamma_\mu \left[ 1 + \delta_{\nu\mu} - \sum_{i=1}^N 2 |\alpha_{\nu,i}|^2 |\alpha_{\mu,i}|^2 \right]}{N^2 \Gamma_0^2} \\ &= \frac{N^2 \Gamma_0^2 + \sum_{\nu=1}^N \Gamma_\nu^2 - 2 \sum_{i=1}^N \left( \sum_{\nu=1}^N \Gamma_\nu |\alpha_{\nu,i}|^2 \right) \left( \sum_{\mu=1}^N \Gamma_\mu |\alpha_{\mu,i}|^2 \right)}{N^2 \Gamma_0^2} \\ &= 1 + \sum_{\nu=1}^N \left( \frac{\Gamma_\nu}{N \Gamma_0} \right)^2 - \frac{2}{N}. \end{aligned} \quad (12)$$



By noting that

$$\frac{1}{N} \text{Var} \left( \frac{\{\Gamma_\nu\}}{\Gamma_0} \right) = \sum_{\nu=1}^N \left( \frac{\Gamma_\nu}{N\Gamma_0} \right)^2 - \frac{1}{N} \quad (13)$$

we recast the expression as

$$g^{(2)}(0) = 1 + \frac{1}{N} \left[ \text{Var} \left( \frac{\{\Gamma_\nu\}}{\Gamma_0} \right) - 1 \right]. \quad (14)$$

## APPENDIX B: DERIVATION OF THE THIRD ORDER CORRELATION FUNCTION $g^{(3)}(0)$

We now consider the third order correlation function, calculated as

$$g^{(2)}(0) = \frac{\sum_{\nu,\mu,\chi=1}^N \Gamma_\nu \Gamma_\mu \Gamma_\chi \langle \hat{\mathcal{O}}_\nu^\dagger \hat{\mathcal{O}}_\mu^\dagger \hat{\mathcal{O}}_\chi^\dagger \hat{\mathcal{O}}_\chi \hat{\mathcal{O}}_\mu \hat{\mathcal{O}}_\nu \rangle}{\left( \sum_{\nu=1}^N \Gamma_\nu \langle \hat{\mathcal{O}}_\nu^\dagger \hat{\mathcal{O}}_\nu \rangle \right)^3}. \quad (15)$$

For the fully-excited state, the denominator is trivially  $(N\Gamma_0)^3$ , while the numerator can be calculated by evaluating the expectation value as

$$\begin{aligned} \langle \hat{\sigma}_{eg}^i \hat{\sigma}_{eg}^j \hat{\sigma}_{eg}^l \hat{\sigma}_{ge}^m \hat{\sigma}_{ge}^n \hat{\sigma}_{ge}^p \rangle &= [\delta_{ip} (\delta_{jn} \delta_{lm} + \delta_{jm} \delta_{ln}) + \delta_{in} (\delta_{jp} \delta_{lm} + \delta_{jm} \delta_{lp}) + \delta_{im} (\delta_{jp} \delta_{ln} + \delta_{jn} \delta_{lp})] \\ &\times (1 - \delta_{ij} - \delta_{il} - \delta_{jl} + 2\delta_{ij} \delta_{il}). \end{aligned} \quad (16)$$

For simplicity, we separate out the calculation into six components  $T_{1-6}$ , each referring to one of the terms in the square brackets above. These are calculated as

$$\begin{aligned} T_1 &= \sum_{i,j,l,m,n,p=1}^N \alpha_{\nu,i}^* \alpha_{\mu,j}^* \alpha_{\chi,l}^* \alpha_{\chi,m} \alpha_{\mu,n} \alpha_{\nu,p} [\delta_{ip} \delta_{jn} \delta_{lm} (1 - \delta_{ij} - \delta_{il} - \delta_{jl} + 2\delta_{ij} \delta_{il})] \\ &= 1 - \sum_{i=1}^N |\alpha_{\mu,i}|^2 |\alpha_{\nu,i}|^2 - \sum_{i=1}^N |\alpha_{\chi,i}|^2 |\alpha_{\nu,i}|^2 - \sum_{j=1}^N |\alpha_{\chi,j}|^2 |\alpha_{\mu,j}|^2 + 2 \sum_{i=1}^N |\alpha_{\chi,i}|^2 |\alpha_{\mu,i}|^2 |\alpha_{\nu,i}|^2, \end{aligned} \quad (17)$$

$$\begin{aligned} T_2 &= \sum_{i,j,l,m,n,p=1}^N \alpha_{\nu,i}^* \alpha_{\mu,j}^* \alpha_{\chi,l}^* \alpha_{\chi,m} \alpha_{\mu,n} \alpha_{\nu,p} [\delta_{ip} \delta_{jm} \delta_{ln} (1 - \delta_{ij} - \delta_{il} - \delta_{jl} + 2\delta_{ij} \delta_{il})] \\ &= \delta_{\mu\chi} - \delta_{\mu\chi} \sum_{i=1}^N |\alpha_{\nu,i}|^2 |\alpha_{\mu,i}|^2 - \delta_{\mu\chi} \sum_{i=1}^N |\alpha_{\nu,i}|^2 |\alpha_{\mu,i}|^2 - \sum_{j=1}^N |\alpha_{\mu,j}|^2 |\alpha_{\chi,j}|^2 + 2 \sum_{i=1}^N |\alpha_{\nu,i}|^2 |\alpha_{\chi,i}|^2 |\alpha_{\mu,i}|^2, \end{aligned} \quad (18)$$

$$\begin{aligned} T_3 &= \sum_{i,j,l,m,n,p=1}^N \alpha_{\nu,i}^* \alpha_{\mu,j}^* \alpha_{\chi,l}^* \alpha_{\chi,m} \alpha_{\mu,n} \alpha_{\nu,p} [\delta_{in} \delta_{jp} \delta_{lm} (1 - \delta_{ij} - \delta_{il} - \delta_{jl} + 2\delta_{ij} \delta_{il})] \\ &= \delta_{\nu\mu} - \sum_{i=1}^N |\alpha_{\nu,i}|^2 |\alpha_{\mu,i}|^2 - \delta_{\nu\mu} \sum_{i=1}^N |\alpha_{\nu,i}|^2 |\alpha_{\chi,i}|^2 - \delta_{\nu\mu} \sum_{j=1}^N |\alpha_{\chi,j}|^2 |\alpha_{\nu,j}|^2 + 2 \sum_{i=1}^N |\alpha_{\chi,i}|^2 |\alpha_{\mu,i}|^2 |\alpha_{\nu,i}|^2, \end{aligned} \quad (19)$$

$$\begin{aligned} T_4 &= \sum_{i,j,l,m,n,p=1}^N \alpha_{\nu,i}^* \alpha_{\mu,j}^* \alpha_{\chi,l}^* \alpha_{\chi,m} \alpha_{\mu,n} \alpha_{\nu,p} [\delta_{in} \delta_{jm} \delta_{lp} (1 - \delta_{ij} - \delta_{il} - \delta_{jl} + 2\delta_{ij} \delta_{il})] \\ &= \delta_{\nu\mu} \delta_{\nu\chi} - \delta_{\nu\chi} \sum_{i=1}^N |\alpha_{\nu,i}|^2 |\alpha_{\mu,i}|^2 - \delta_{\mu\chi} \sum_{i=1}^N |\alpha_{\nu,i}|^2 |\alpha_{\mu,i}|^2 - \delta_{\nu\mu} \sum_{j=1}^N |\alpha_{\nu,j}|^2 |\alpha_{\chi,j}|^2 + 2 \sum_{i=1}^N |\alpha_{\chi,i}|^2 |\alpha_{\mu,i}|^2 |\alpha_{\nu,i}|^2, \end{aligned} \quad (20)$$

$$\begin{aligned}
T_5 &= \sum_{i,j,l,m,n,p=1}^N \alpha_{\nu,i}^* \alpha_{\mu,j}^* \alpha_{\chi,l}^* \alpha_{\chi,m} \alpha_{\mu,n} \alpha_{\nu,p} [\delta_{im} \delta_{jp} \delta_{ln} (1 - \delta_{ij} - \delta_{il} - \delta_{jl} + 2\delta_{ij} \delta_{il})] \\
&= \delta_{\nu\mu} \delta_{\nu\chi} - \delta_{\mu\chi} \sum_{i=1}^N |\alpha_{\nu,i}|^2 |\alpha_{\mu,i}|^2 - \delta_{\nu\mu} \sum_{i=1}^N |\alpha_{\nu,i}|^2 |\alpha_{\chi,i}|^2 - \delta_{\nu\chi} \sum_{j=1}^N |\alpha_{\mu,j}|^2 |\alpha_{\nu,j}|^2 + 2 \sum_{i=1}^N |\alpha_{\nu,i}|^2 |\alpha_{\chi,i}|^2 |\alpha_{\mu,i}|^2, \quad (21)
\end{aligned}$$

$$\begin{aligned}
T_6 &= \sum_{i,j,l,m,n,p=1}^N \alpha_{\nu,i}^* \alpha_{\mu,j}^* \alpha_{\chi,l}^* \alpha_{\chi,m} \alpha_{\mu,n} \alpha_{\nu,p} [\delta_{im} \delta_{jn} \delta_{lp} (1 - \delta_{ij} - \delta_{il} - \delta_{jl} + 2\delta_{ij} \delta_{il})] \\
&= \delta_{\nu\chi} - \delta_{\nu\chi} \sum_{i=1}^N |\alpha_{\nu,i}|^2 |\alpha_{\mu,i}|^2 - \sum_{i=1}^N |\alpha_{\nu,i}|^2 |\alpha_{\chi,i}|^2 - \delta_{\nu\chi} \sum_{j=1}^N |\alpha_{\mu,j}|^2 |\alpha_{\nu,j}|^2 + 2 \sum_{i=1}^N |\alpha_{\nu,i}|^2 |\alpha_{\mu,i}|^2 |\alpha_{\chi,i}|^2. \quad (22)
\end{aligned}$$

We sum these to find  $g^{(3)}(0)$  as

$$\begin{aligned}
g^{(3)}(0) &= \frac{1}{N^3 \Gamma_0^3} \sum_{\nu=1}^N \sum_{\mu=1}^N \sum_{\chi=1}^N \Gamma_\nu \Gamma_\mu \Gamma_\chi \left( 1 + 2\delta_{\nu\mu\chi} + \delta_{\nu\mu} + \delta_{\nu\chi} + \delta_{\mu\chi} + 12 \sum_{i=1}^N |\alpha_{\nu,i}|^2 |\alpha_{\mu,i}|^2 |\alpha_{\chi,i}|^2 \right. \\
&\quad - 2 \sum_{i=1}^N |\alpha_{\nu,i}|^2 |\alpha_{\chi,i}|^2 - 2 \sum_{i=1}^N |\alpha_{\nu,i}|^2 |\alpha_{\mu,i}|^2 - 2 \sum_{i=1}^N |\alpha_{\mu,i}|^2 |\alpha_{\chi,i}|^2 \\
&\quad \left. - 4\delta_{\nu\chi} \sum_{i=1}^N |\alpha_{\nu,i}|^2 |\alpha_{\mu,i}|^2 - 4\delta_{\nu\mu} \sum_{i=1}^N |\alpha_{\nu,i}|^2 |\alpha_{\chi,i}|^2 - 4\delta_{\mu\chi} \sum_{i=1}^N |\alpha_{\nu,i}|^2 |\alpha_{\mu,i}|^2 \right) \\
&= \frac{1}{N^3 \Gamma_0^3} \left( N^3 \Gamma_0^3 + 2 \sum_{\nu=1}^N \Gamma_\nu^3 + 3N\Gamma_0 \sum_{\nu=1}^N \Gamma_\nu^2 + 12N\Gamma_0^3 - 6N^2\Gamma_0^3 - 12\Gamma_0 \sum_{\nu=1}^N \Gamma_\nu^2 \right) \\
&= 1 + 2 \sum_{\nu=1}^N \left( \frac{\Gamma_\nu}{N\Gamma_0} \right)^3 + \left( 3 - \frac{12}{N} \right) \sum_{\nu=1}^N \left( \frac{\Gamma_\nu}{N\Gamma_0} \right)^2 + \frac{12}{N^2} - \frac{6}{N}. \quad (23)
\end{aligned}$$